Delineation of mRNA Export Pathways by the Use of Cell-Permeable Peptides

Imed-Eddine Gallouzi* and Joan A. Steitz†

The transport of messenger RNAs (mRNAs) from the nucleus to the cytoplasm involves adapter proteins that bind the mRNA as well as receptor proteins that interact with the nuclear pore complex. We demonstrate the utility of cell-permeable peptides designed to interfere with interactions between potential adapter and receptor proteins to define the pathways accessed by particular mRNAs. We show that HuR, a protein implicated in the stabilization of short-lived mRNAs containing AU-rich elements (AREs), serves as an adapter for *c-fos* mRNA export through two pathways. One involves the HuR shuttling domain, HNS, which exhibits a heat shock–sensitive interaction with transportin 2 (Trn2); the other involves two protein ligands of HuR—pp32 and APRIL—which contain leucine-rich nuclear export signals (NES) recognized by the export receptor CRM1. Heterokaryon and in situ hybridization experiments reveal that the peptides selectively block the nucleocytoplasmic shuttling of their respective adapter proteins without perturbing the overall cellular distribution of polyadenylated mRNAs.

Transport from the nucleus to the cytoplasm of both proteins and RNAs occurs through the nuclear pore complex (NPC) (*1–5*). The process is mediated by saturable export receptor proteins that recognize signals on cargo molecules, that interact directly with NPC components, and that shuttle continuously between the nucleus and the cytoplasm. For mRNA, maturation and transport are tightly coupled, such that splicing, polyadenylation, and capping all affect export. These processing events are believed to be accompanied by the deposition of adapter proteins on nascent transcripts (*6–9*) to form export-competent ribonucleoproteins. The adapters in turn interact with export receptors, enabling mRNA transit through the pore.

Currently, the best characterized mammalian export receptor is CRM1 (chromosome maintenance region 1), which associates with its cargo by recognizing a leucine-rich nuclear export signal (NES) of only about 10 amino acids (*10–12*). CRM1 is known to regulate the export of unspliced human immunodefiency virus–1 (HIV-1) RNA, U snRNAs, and the yeast 60*S* ribosomal subunit through the NES-containing adapter proteins, HIV-1 Rev, PHAX, and Nmd3p, respectively (*13–15*).

Department of Molecular Biophysics and Biochemistry, Howard Hughes Medical Institute, Yale University School of Medicine, 295 Congress Avenue, New Haven, CT 06536, USA.

*Present address: Department of Biochemistry, McGill University, McIntyre Medical Sciences Building, 3655 Promenade Sir William Osler, Montreal, Quebec H3G 1Y6, Canada.

†To whom correspondence should be addressed: E-mail: joan.steitz@yale.edu

Receptors and adapters for the export of cellular mRNAs have remained less well defined. HnRNP A1 is a putative adapter protein (*16*), whose nucleocytoplasmic shuttling is conferred by a 38–amino acid domain named M9 located in its COOH-terminus (*17*, *18*). The M9 motif interacts with the receptor transportin 1 (Trn1), a member of the importin β family that functions in both the nuclear import and export of hnRNP A1 (*19*, *20*). HnRNP A1 has been implicated in the nuclear export of the dihydrofolate reductase (DHFR) mRNA in *Xenopus* oocyte experiments (*21*). Other shuttling, RNA-binding proteins that are considered potential adapters are hnRNP K, SRP20, 9G8, and ASF/SF2 (*22–25*). The TAP receptor, which uses the Aly/REF proteins as adapters, is known to play a major role in the export of cellular mRNAs (*8*, *9*, *26–30*). However, because many potential adapters bind to each mammalian mRNA, it has not been possible to identify the adapter-receptor pair(s) responsible for orchestrating the export of individual mRNAs.

The mRNAs of early response genes (ERGs) encode key growth-regulatory proteins such as cytokines, lymphokines, and protooncogenes and are typically short-lived, allowing rapid shut-off as well as induction of their expression (*31*, *32*). They contain AU-rich elements (AREs) in their 3′ untranslated regions (UTRs) (*33*, *34*) that interact with numerous proteins to regulate their cellular half-lives (*33–36*). One such protein is HuR, a ubiquitously expressed member of the embryonic lethal abnormal vision (ELAV) family of RNA-binding proteins (*37*). Its overexpression in transiently transfected mammalian cells leads to the stabilization of reporter mRNAs carrying AREs (*38*, *39*). Like other members of the ELAV family, HuR contains three RNA recognition motifs (RRM). Although HuR appears nuclear, it continuously shuttles between the nucleus and cytoplasm directed by a sequence designated HNS (HuR Nucleocytoplasmic Shuttling) located in the 52–amino acid hinge region between RRM2 and RRM3 (*38*). Systematic deletion analyses demonstrated that HNS comprises 33 amino acids, which do not appear to correspond to any previously described class of shuttling motifs (*40*). We recently showed that HuR associates with abundant nuclear phosphoprotein ligands called pp32 and APRIL (*41*, *42*), which likewise shuttle, but through leucine-rich NES domains (*43*). Inhibition of the CRM1 nuclear export pathway with the inhibitor leptomycin B (LMB) (*10*) blocks the shuttling of pp32 and APRIL but does not appear to affect HuR cellular movement (*43*). Yet, after treatment with LMB, ultraviolet (UV) cross linking of HuR to polyadenylated [poly(A)$^+$] RNA is detected in both the nucleus and the cytoplasm, whereas this association [HuR with poly(A)$^+$ RNA] occurs exclusively in the cytoplasm under normal conditions (*43*, *44*), and *c-fos* mRNA, an HuR-bound ERG message (*37*, *45–47*), becomes restricted to the nucleus (*43*). These observations suggested that HuR might access two alternative pathways for nuclear export, one CRM1-dependent (involving its ligands pp32 and APRIL) and the other CRM1-independent (using its endogenous HNS shuttling sequence).

To investigate the possibility that HuR serves as an export adapter protein for ERG mRNAs and to characterize molecular interactions underlying its nucleocytoplasmic transport, we sought a way to interfere selectively with individual nuclear export pathways in living cells. Previously, NES peptides coupled to various carrier proteins have been microinjected into *Xenopus* oocytes (*48*, *49*) to study the nuclear export of mRNAs and other classes of cellular RNAs. The difficulty with applying similar approaches to intact mammalian cells has been how to deliver such inhibitors with high efficiency. Here, we optimized the use of cell-permeable peptides (*50–54*) designed to inhibit interactions between particular receptor and adapter protein pairs. Effects are seen in close to 100% of mammalian cells in culture. By examining endogenous mRNAs, we have begun to identify the pathways that are dominant in the export of specific messages to the cytoplasm.

Selective inhibition of mRNA export and protein shuttling by peptide inhibitors. We synthesized peptides corresponding to known export or shuttling domains of

candidate adapter proteins (the NES, M9, and HNS sequences) as COOH-terminal fusions to a portion of the homeodomain of Antennapedia, a *Drosophila* transcription factor (Fig. 1A). This 16–amino acid sequence (here designated AP) facilitates the homogeneous uptake of peptides into cultured mammalian cells through a nonendocytic, nondegradative pathway with 100% efficiency (*51–53*). Control peptides (Fig. 1A) were of the same length and amino acid composition but were scrambled in sequence (scHNS and scM9) or, in the case of NES, contained Leu → Ala mutations at two sites known to be essential for NES function (*55*, *56*). The effect of these peptides on cell viability was assessed by incubating them at 25 μM with cultured HeLa cells. The cells grew normally with the AP-mNES, AP-scM9, or AP-scHNS peptide for at least 72 hours, whereas 50% of the cells died after 36 hours with AP-NES, AP-M9, or AP-HNS. Nonetheless, cell growth and viability appeared unchanged for the first 24 hours (*57*); if the inhibitory peptide was removed after 12 hours, the cells were able to recover. We examined cellular uptake using rhodamine-labeled AP peptides and observed that all peptides tested appeared in both the cytoplasm and nucleus in less than 15 min (*57*).

We first validated use of the peptides for studying mRNA export by probing the interaction of the HIV-1 Rev protein (containing an NES) with its receptor CRM1. The Rev protein functions as an export adapter by recognizing the Rev responsive element (*RRE*) within a target RNA (*13*). We expressed in HeLa cells an *RRE*-containing reporter (*RRE*) with or without HIV-1 Rev (*58–60*). As expected, in situ hybridization (*61*) with a digoxigenin-labeled complementary oligonucleotide (Fig. 1B) showed that after 24 hours, *RRE* was confined to the nucleus (panel 1) but became detectable in the cytoplasm as well when coexpressed with the HIV-1 Rev protein (panel 2). Treating the cells in panel 2 with different peptides for 4 hours before analysis confirmed that AP-NES (panel 3) but not AP-mNES (panel 4) blocked the

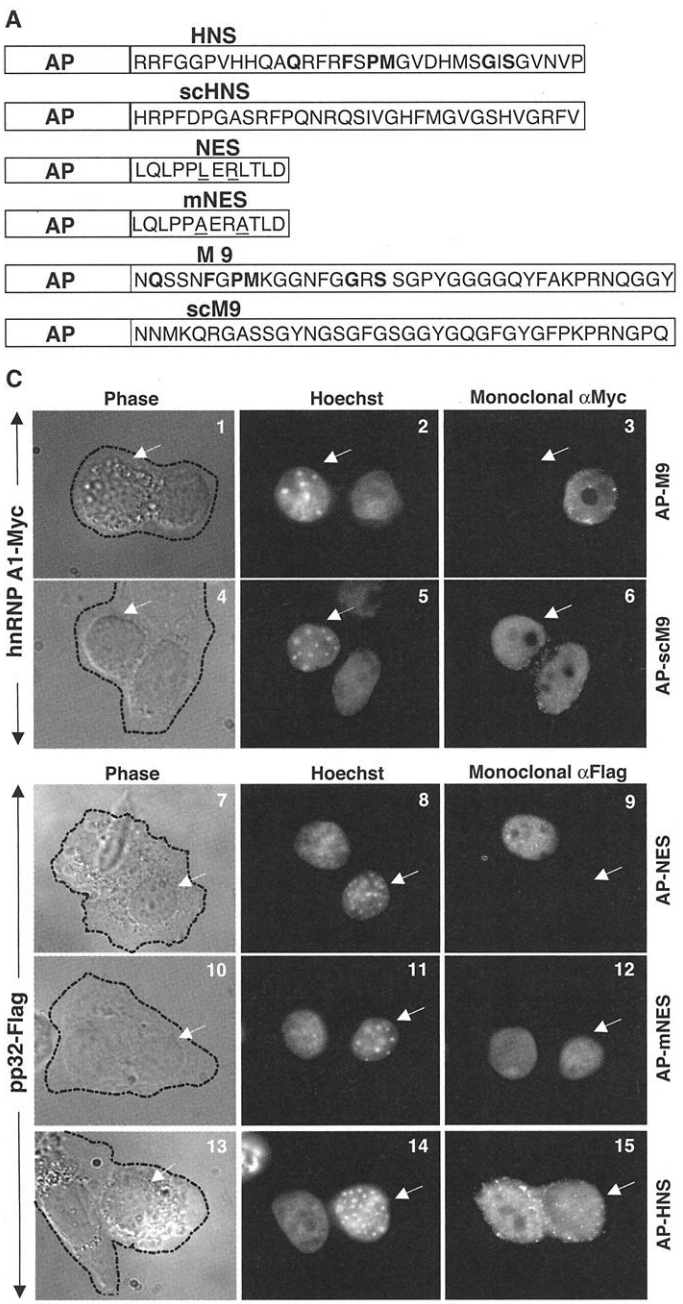

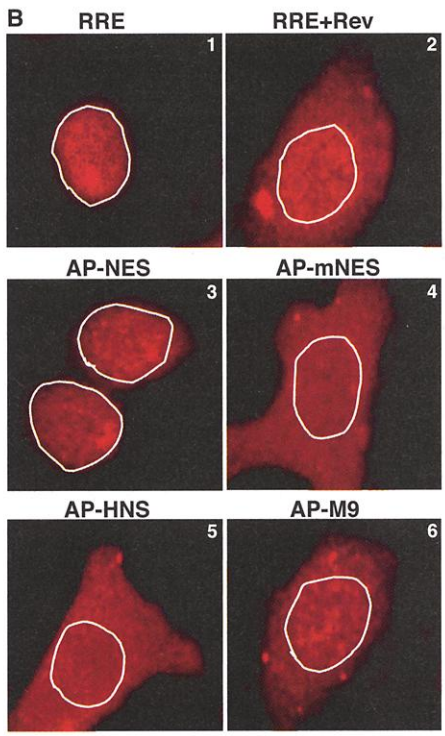

Fig. 1. Validation of the use of cell-permeable peptides to study mRNA nuclear export and protein shuttling. (**A**) Each peptide (*77*) contained at its NH_2-terminus the antennapedia internalization element (AP = RQIKIWFQNRRMKWKK) (*78*) followed by HNS (amino acids 205 to 237 of HuR) (*40*), NES (amino acids 73 to 84 of Rev) (*10*, *48*, *49*, *79*), M9 (amino acids 268 to 305 of hnRNP A1) (*18*), a scrambled (sc) HNS or M9 sequence, or a mutant (m) NES with leucines 78 and 81 replaced by alanines (underlined residues) (*55*, *56*). Amino acids conserved in M9 domains (*66*) that are also common to HNS are shown in bold (*40*). (**B**) AP-NES inhibits the export of an *RRE*-containing reporter RNA. HeLa cells were grown on cover slips (*80*), transfected either with pDM128 containing the HIV-1 *RRE* inserted into CAT cDNA (*59*, *60*) (panel 1) or with both pDM128 and pRSV-Rev (*59*, *60*) (panels 2 to 6) plasmids for 24 hours. After 4 hours with an AP peptide (25 μM), *RRE* was localized by in situ hybridization (*61*). The dotted lines indicating nuclear boundaries were constructed from the phase images of the same cells, which also revealed that cell shape and integrity were maintained. (**C**) Inhibition of hnRNP A1 and pp32 nucleocytoplasmic shuttling by AP-M9 and AP-NES, respectively. Heterokaryons of HeLa and mouse L929 cells were formed as described (*18*, *40*) with some modifications (*63*) because of exposure to the indicated AP peptides. Fixed cells were stained with either monoclonal antibody to Flag (M2) (for pp32) or monoclonal antibody to Myc (9E10) (for hnRNP A1) (Sigma-Aldrich). Cells were also stained with Hoechst 33258 (Sigma-Aldrich) to distinguish the human and mouse nuclei. The (speckled) mouse nucleus in each field is indicated by an arrow. The heterokaryons are outlined with dashed lines in the phase images. The results in (B) and (C) were repeated five times, with greater than 95% of cells appearing like those presented.

export of *RRE* from the HeLa nucleus to the cytoplasm. Neither AP-M9 nor AP-HNS inhibited the cytoplasmic appearance of *RRE* (panels 5 and 6), demonstrating that only the peptide designed to compete with the NES-CRM1 interaction interferes with *RRE* export.

We next asked whether peptides would similarly block the well-characterized nucleocytoplasmic shuttling of the putative export adapter protein hnRNP A1 (*17*), as well as that of the HuR ligand pp32 (*43*). Using the transient transfection interspecies heterokaryon assay previously described (*38*), we added peptides for 4 hours, starting 1 hour before initiating cell fusion. We observed that the migration of hnRNP A1-Myc from the human nucleus (uniform staining by Hoechst; Fig. 1C, panels 2 and 5) to the mouse nucleus (spotted staining, indicated by arrows) was inhibited by AP-M9, but not by AP-scM9 (panels 3 and 6).

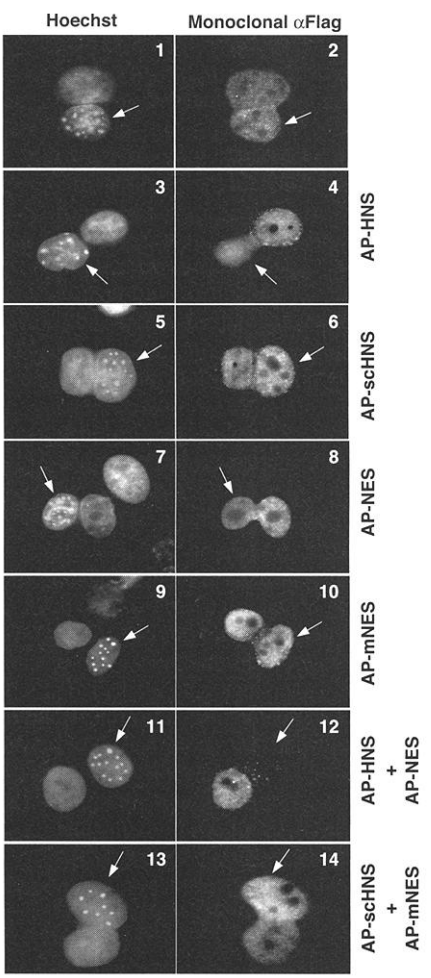

Fig. 2. The AP-HNS and AP-NES peptides together inhibit HuR nucleocytoplasmic shuttling. Treatment with the indicated AP peptide(s) and the heterokaryon assay were performed as described in Fig. 1C, after transfection of HeLa cells with the Flag-HuR plasmid (*40*). Panels 1 and 2 show a heterokaryon not treated with peptide.

This confirms that the M9 domain (*18*) is essential for hnRNP A1 shuttling in vivo. Shuttling of pp32 had previously been shown to be sensitive to LMB (*43*), which prevents the association of the required cofactor Ran–guanosine triphosphate (Ran-GTP) with CRM1 (*11*, *62*). Accordingly, AP-NES completely blocked pp32 shuttling (Fig. 1C, panel 9). In contrast, AP-mNES (panel 12), which is altered in only two amino acids (Fig. 1A), had no effect, nor did AP-HNS (Fig. 1C, panel 15) or AP-M9 (*57*), further confirming the specificity of the peptides. This experiment also indicates the utility of AP-NES as a substitute for LMB in functional assays of the CRM1 receptor.

HNS and NES peptides block HuR shuttling and alter HuR interaction with poly(A)$^+$ RNA. To explore the in vivo pathway(s) responsible for HuR nucleocytoplasmic shuttling, we used AP peptides in the heterokaryon assay (*63*) with HeLa cells expressing HuR-Flag (*38*). Simultaneous exposure to AP-HNS and AP-NES completely blocked HuR movement (Fig. 2, panel 12). Individually, these peptides showed only a very weak (AP-HNS, panel 4) or no effect (AP-NES, panel 8) on HuR appearance in the mouse nucleus. In control experiments, we observed HuR shuttling without any treatment (panel 2) or in the presence of AP-scHNS (panel 6), AP-mNES (panel 10), or a combination of these two peptides (panel 14). These observations suggest the existence of two and only two pathways for HuR nuclear export under the conditions assayed.

To determine the involvement of these two pathways in the potential function of HuR as an adapter protein for the export of ARE-containing mRNAs, we first performed in vivo UV cross linking on HeLa cells (*64*) in the presence or absence of AP peptides (Fig. 3). The covalent attachment of HuR and hnRNP A1 to poly(A)$^+$ RNA isolated from the nuclear and cytoplasmic fractions was demonstrated by probing immunoblots with monoclonal antibodies to HuR (*44*) and hnRNP A1 (*17*). In the absence of peptides, HuR cross linked to poly(A)$^+$ RNA only in the cytoplasmic compartment (Fig. 3, compare lanes 4 and 5), as observed previously (*44*). Together, the AP-HNS and the AP-NES peptides led to a complete shift of HuR interactions to nuclear poly(A)$^+$ RNA (lanes 14 and 15), whereas individually these two peptides induced only a partial shift from the cytoplasm to the nucleus (lanes 6 and 7 and 10 and 11). Neither the AP-scHNS, AP-mNES, nor AP-M9 peptide, alone or in combination, affected HuR cross linking (lanes 8 and 9, 12 and 13, 16 and 17, and 18 and 19). These peptide inhibitors had no effect on hnRNP A1 association with poly(A)$^+$ RNA, which remained completely nuclear (lanes 4 to 19). These results are compatible with the idea that HuR normally binds its target mRNAs just before exit from the nucleus (*44*); if its export is blocked by peptides, HuR is seen cross linked to nuclear poly(A)$^+$ RNA. Thus, HuR could be an adapter protein escorting at least some ARE-containing mRNAs from the nucleus to the cytoplasm using both the NES-dependent and HNS-dependent pathways.

Selective peptide inhibition of *c-fos* and DHFR mRNA export. The *c-fos* ERG mRNA is an ARE-containing message that binds HuR (*37*, *39*, *45*–*47*). HeLa cells were serum stimulated to increase their *c-fos* production to detectable levels (*65*) and treated with AP peptides. Visualization of *c-fos* mRNA by in situ hybridization (Fig. 4) revealed that the same two peptides that inhibit HuR shuttling and shift its binding to only nuclear poly(A)$^+$ RNA lead to complete sequestration of *c-fos* mRNA in the nucleus (panel 5). AP-HNS alone had only a slight effect on *c-fos* cellular distribution (panel 1), whereas AP-NES induced substantial, but not complete retention of *c-fos* mRNA in the nucleus (panel 3). The AP-scHNS, AP-mNES, AP-M9, and AP-scM9 peptides served as negative controls (panels 2, 4, and 6 to 8). This inhibition

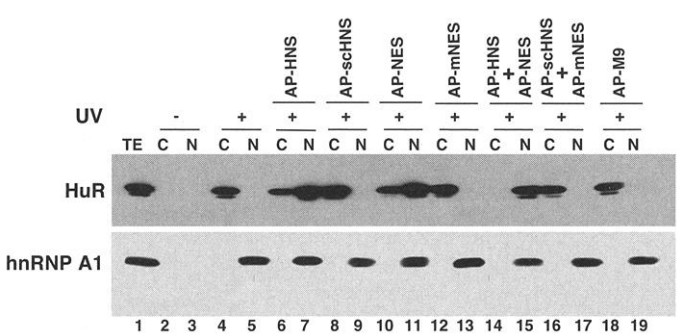

Fig. 3. The AP-HNS and AP-NES peptides together shift HuR interactions with poly(A)$^+$ RNA from the cytoplasm to the nucleus. HeLa cells were incubated in the absence (lanes 2 to 5) or the presence of the indicated AP peptides (lanes 6 to 19) and exposed (lanes 4 to 19) or not (lanes 2 and 3) to UV light, and proteins cross linked to poly(A)$^+$ RNA in the cytoplasmic (C) and nuclear (N) fractions (*17*, *64*) were detected by Western blot (*44*). Lanes labeled (−) were treated with neither UV light nor AP peptide. TE (lane 1) shows total extract from 1/100 the number of cells analyzed in the C + N lanes.

provides evidence that both the HNS- and NES-dependent pathways are involved in *c-fos* mRNA nuclear export, with a preference for the NES-dependent route.

In contrast to *c-fos* mRNA, the nuclear retention of DHFR mRNA requires only a single AP peptide. Complete blockage of DHFR mRNA export with AP-M9 (Fig. 4, panel 11) confirms for mammalian cells earlier experiments in *Xenopus* oocytes showing the involvement of hnRNP A1 (*21*). The control AP-HNS, AP-NES, and AP-scM9 peptides had no effect on DHFR mRNA cellular localization (panels 9, 10, and 12).

Because the peptides appeared so selective in their inhibition of the export of particular mRNAs, we also assessed the distribution of total poly(A)$^+$ RNA using an oligo(dT) probe (Fig. 4, panels 13 to 20). Previously, blocking the CRM1 pathway with LMB was observed to have no effect on poly(A)$^+$ RNA cellular distribution (*43*). The observation that no single peptide or even combinations of two peptides (panels 17 and 18) substantially lowered the cytoplasmic signal argues that multiple pathways contribute to the nuclear export of mammalian mRNAs.

The HNS domain of HuR exhibits a heat-sensitive interaction with transportin 2. Because the nuclear export of HuR and at least one ARE-containing mRNA is inhibited by a cell-permeable peptide corresponding to the HNS domain, it was of great interest to identify the export receptor that recognizes this shuttling motif (*40*). When characterizing transportin 1 (Trn1), Siomi *et al.* identified transportin 2 (Trn2), which is 84% identical to Trn1 but does not interact with hnRNP A1 (*20*), suggesting that it may be a receptor for an as yet unidentified adapter protein. Although HNS is not strikingly homologous to the M9 domain of hnRNP A1, they share several amino acids that have been identified as conserved in M9 motifs across species (Fig. 1A, bold residues) (*40*, *66*). We therefore suspected that Trn2, which is related to the M9 receptor Trn1 (*20*), might recognize HNS.

We first performed far-Western blotting experiments by transferring glutathione S-tranferase (GST)–tagged HuR, Trn1, Trn2, and pp32 proteins (*67*) to a nitrocellulose membrane and probing with either ^{35}S-Met–labeled HuR (^{35}S-HuR) or HNS (^{35}S-HNS) (Fig. 5A). We observed that ^{35}S-HuR interacted specifically with GST-Trn2, but not with GST-Trn1 (compare lanes 3 and 4), as did the 33–amino acid ^{35}S-HNS (lanes 8 and 9). ^{35}S-HuR also interacted with its protein ligand, GST-pp32 (lane 5), whereas ^{35}S-HNS bound only weakly (lane 10), as reported previously (*43*). In contrast, ^{35}S-hnRNP A1 interacted with GST-Trn1, but not with GST-Trn2 (lanes 13 and 14), as expected (*20*). The same GST-tagged proteins were purified on glutathione Sepharose, packed into a column, and exposed either to ^{35}S-HuR or ^{35}S-HNS (lanes 17 to 21) or to ribonuclease A (RNase A)–treated HeLa whole-cell extract (*43*) followed by immunoblotting (lanes 23 to 27). These affinity experiments (Fig. 5A, lanes 16 to 27) confirmed those described above, revealing the specific interaction of Trn2 with HuR through its HNS domain.

To ask whether HuR-Trn2 interactions could also be demonstrated in cell extracts, we performed immunoprecipitation experiments on RNase A–treated total HeLa cell extract using either polyclonal antibody to Trn2 (*68*) or monoclonal antibody to HuR (*44*). HuR was specifically coimmunoprecipitated by the antibody to Trn2 (Fig. 5B, lane 6), and, conversely, the antibody to HuR immunoprecipitated Trn2 (lane 3). Moreover, a monoclonal antibody to HuR did not immunoprecipitate Trn1 (Fig. 5C, lane 3), whereas a monoclonal antibody to Trn1 [D45 (*20*)] precipitated Trn1 with high efficiency (lane 5).

Identification of Trn2 as the receptor for HNS also allowed us to confirm that the AP-HNS peptide specifically blocks the interaction between an adapter (HuR) and receptor protein (Trn2) in vivo. We treated HeLa cells for 4 hours with various AP peptides, prepared RNase-treated total extracts, and performed immunoprecipitation using polyclonal antibodies to Trn2, pp32, and APRIL (Fig. 5D). Western blotting of the precipitates with the monoclonal antibody to HuR showed that only the AP-HNS peptide abolished HuR association with Trn2 (Fig. 5D, compare lane 1 with lanes 2 to 12). Moreover, when the same blot was probed with a polyclonal antibody to CRM1 (*11*), we observed that the AP-NES peptide disrupted CRM1-pp32 and CRM1-APRIL associations (*57*) without affecting the HuR-Trn2 complex. Together, these observations argue that HuR through its HNS motif interacts with Trn2 in vivo.

Alternative export routes for an mRNA adapter protein might facilitate cellular adjustment to changing conditions. We previously observed that upon heat shock, HuR shuttling between the nucleus and the cytoplasm switches exclusively to the CRM1 pathway, apparently involving HuR ligands pp32 and APRIL (*69*). This observation suggested that HuR's interaction with Trn2 may be heat sensitive, resulting in the loss of this export pathway. We therefore performed im-

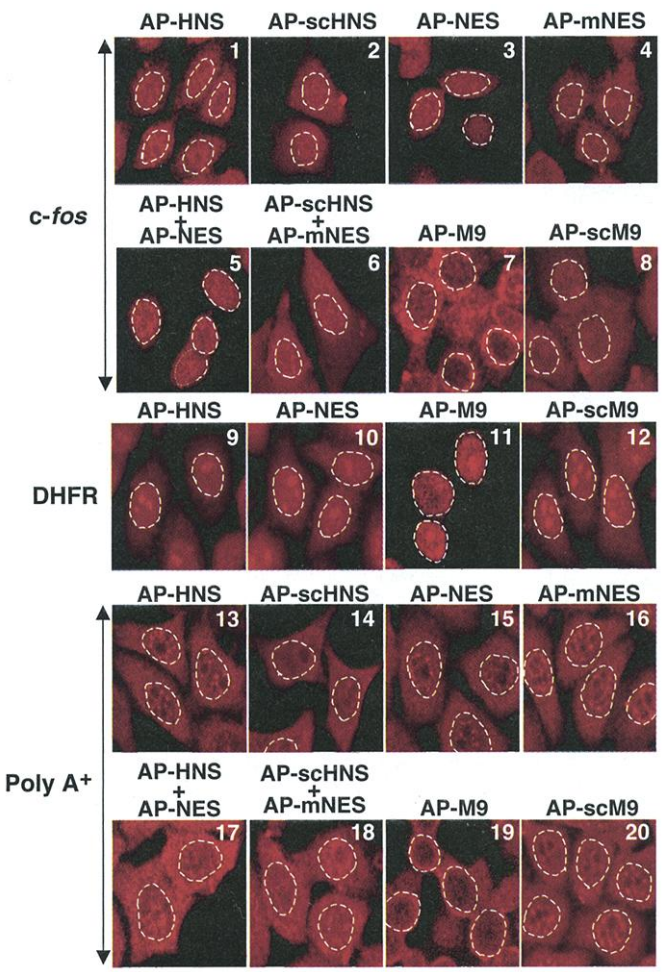

Fig. 4. Selective inhibition of *c-fos* and DHFR mRNA export by AP peptides. HeLa cells were induced for *c-fos* expression (*81*) (panels 1 to 8) or not (panels 9 to 20), treated with the indicated AP peptide or a mixture of two peptides for 4 hours as described in Fig. 1B, fixed, and subjected to in situ hybridization (*61*) with antisense probes for *c-fos*, DHFR, or oligo(dT)$_{40}$ (*82*). A mixture of NES, HNS, and M9 peptides produced the same poly(A)$^+$ pattern as in panel 19 (M9 alone) (*57*).

munoprecipiation experiments on RNase-treated extract from HeLa cells exposed to 45°C for 1 hour (*44*, *69*) using the antibody to Trn2 for precipitation and the monoclonal antibody to HuR for Western blotting. Figure 6A (lanes 2 and 3) shows that HuR-Trn2 association is indeed completely abolished after heat shock. Lack of interaction could be explained if heat shock perturbed the cellular localization of either of the two proteins such that they no longer coexist in the nuclear compartment. Thus, we assessed Trn2 cellular distribution before and after heat shock by immunofluorescence using the polyclonal antibody to Trn2 (Fig. 6B, panels 1 and 2). Both sets of cells exhibited the same primarily nuclear localization for Trn2. Because 85% of HuR also remains nuclear after heat shock (*44*), the lack of interaction between HuR and its export receptor Trn2 (Fig. 6A) probably results from some as yet uncharacterized modification (including heat-induced conformational change) of one or both proteins.

Two pathways for HuR nucleocytoplasmic movement. We provide evidence that Trn2, a previously an unassigned transport receptor, specifically interacts with the HNS shuttling domain of HuR. The results of our far-Western experiments make this likely to be a direct contact rather than one mediated by other cellular proteins. We do not yet know whether Trn2 is also active in the nuclear import of HuR and whether shuttling is Ran-dependent, but by analogy to Trn1 (*19*, *20*), we expect so. Certainly, HNS exhibits the same bidirectional movement and sensitivity to transcription inhibitors (*40*) as M9 (*18*).

Yet, the inhibition pattern with cell-permeable peptides (Fig. 2) shows that HNS-Trn2 is not the only adapter-receptor pair active in the export of HuR to the cytoplasm. Through association with its protein ligands, pp32 and APRIL, HuR accesses the CRM1 pathway (*69*). Our previous analysis of the sequences required for HuR interaction with its ligands revealed that both RRM3 and the HNS domain of HuR are essential for efficient ligand binding (*43*). Therefore, it is

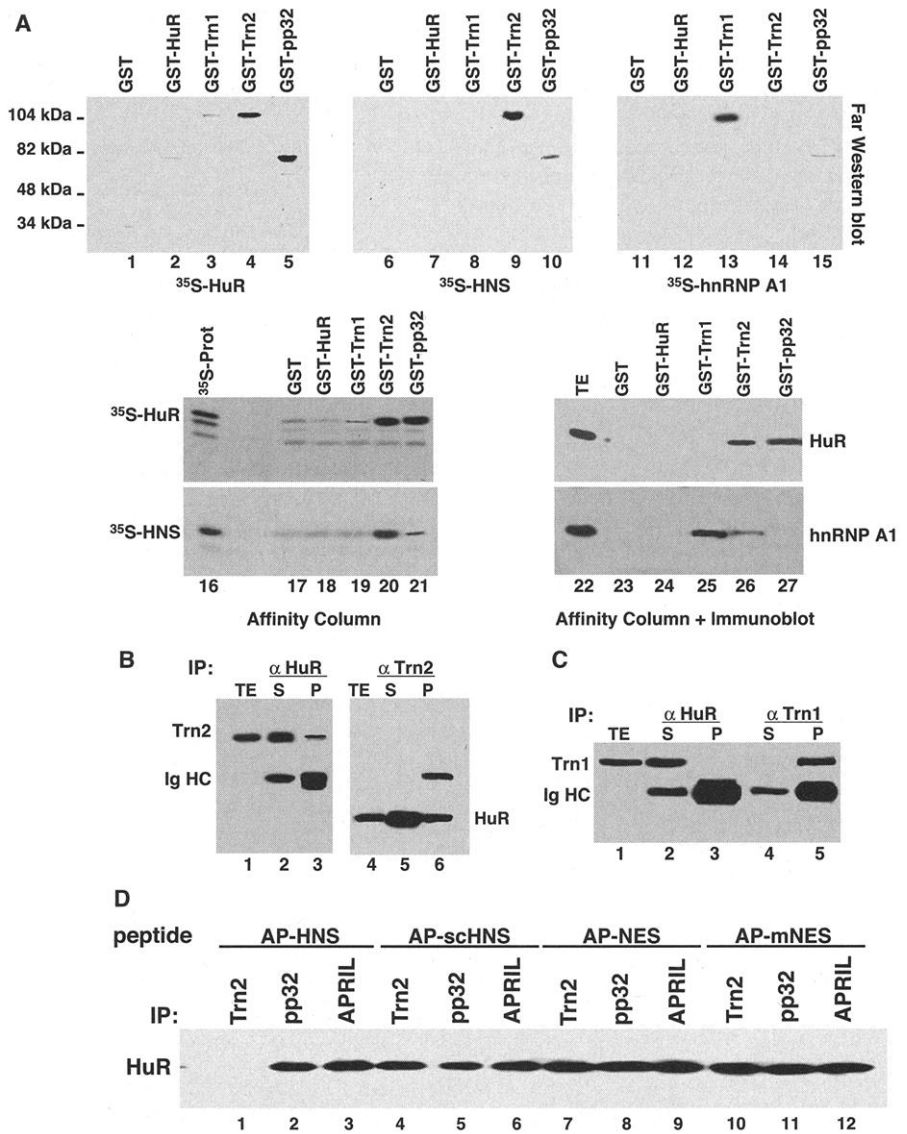

Fig. 5. HuR interacts with transportin 2 through its HNS domain. (**A**) In vitro binding of transportin 2 (Trn2) to HuR is mediated by HNS. Purified recombinant GST, GST-HuR (*43*), GST–transportin 1 (GST-Trn1) (*19*), GST–transportin 2 (GST-Trn2) (*20*), and GST-pp32 (*43*, *67*) were transferred to nitrocellulose after 10% SDS–polyacrylamide gel electrophoresis (SDS-PAGE) and probed with in vitro translated ^{35}S-labeled full-length HuR, HNS (HuR amino acids to 205 to 237), or hnRNP A1 (*83*). For the two bottom panels (lanes 16 to 27), 10 μg each of the above GST or GST fusion proteins were bound to glutathione-Sepharose beads (Pharmacia) (*84*), incubated with either ^{35}S-HuR or ^{35}S-HNS as above or RNase-treated HeLa cell extract (from 10^7 cells), and analyzed as described (*43*). Lanes 16 and 22 contain 10% of the total labeled protein and 10% of the total extract used, respectively. (**B** and **C**) HuR interacts with Trn2, but not with Trn1 in cell extracts. TE lanes show 10% of the total extract (from 10^7 cells) used in adjacent lanes. Immunoprecipitations were performed and analyzed (*43*) with the antibodies described (*68*). Ig HC stands for immunoglobulin heavy chain. P, pellet; S, supernatant. (**D**) HuR interaction with Trn2 in vivo is abolished only by AP-HNS. 10^7 HeLa cells were treated for 4 hours with AP-HNS, AP-scHNS, AP-NES, or AP-mNES, and cell extracts were prepared, immunoprecipitated, and analyzed as described (*43*).

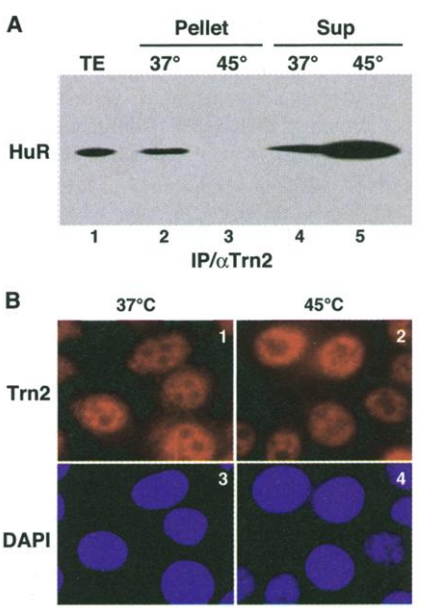

Fig. 6. Heat shock abolishes HuR–transportin 2 association in vivo without altering Trn2 nuclear localization. (**A**) RNase A–treated total extract from 2×10^7 HeLa cells grown at 37°C or exposed to 45°C for 1 hour was prepared, immunoprecipitated (*68*), and analyzed as described (*43*). TE (lane 1) shows 10% of the extract used in the remaining lanes. (**B**) HeLa cells grown on glass cover slips (*80*) were fixed and permeabilized before (panels 1 and 3) or after exposure to 45°C for 1 hour (panels 2 and 4) as described (*38*) and probed (*69*) with αTrn2 (1:300 dilution) (panels 1 and 2) and DAPI (4′, 6′-diamidino, 2-phenylindole) (panels 3 and 4).

likely that interaction with Trn2 and a ligand are mutually exclusive, meaning that a single HuR molecule (depending on its liganded state) can use only one export pathway.

Our results further argue that HuR, previously assigned a role in the stabilization of ERG mRNAs through its binding to AREs in their 3′ UTRs (*38*, *39*), also serves as the dominant export adapter for this important class of mRNAs. Formally, it is possible that the export of HNS- and NES-containing adapter proteins other than HuR and its ligands is being inhibited by the AP-HNS and AP-NES peptides to yield nuclear retention of the *c-fos* mRNA (Fig. 4). An alternative possibility is that the AP peptides inhibit some upstream process such as splicing or polyadenylation, which are required for transport; this is unlikely because Northern blotting revealed that the *c-fos* (and DHFR) mRNA in peptide-treated cells is identical in size and level to that in untreated cells (*57*). Thus, the simplest hypothesis to explain why HuR protein shuttling and *c-fos* mRNA export respond identically to inhibitory peptides is that HuR is the critical export adapter protein. We have also observed that the export of two other ARE-containing mRNAs encoding the E6 and E7 proteins of human papilloma virus 18 (*70*, *71*) (which are endogenous in HeLa cells) is sensitive to inhibition of the CRM1 pathway with LMB (*57*). Perhaps access to two distinct mRNA export pathways enhances the rapid expression of ERG proteins, thereby providing a prompt cellular response to a variety of external stimuli (*31*, *32*, *69*, *72*, *73*).

Another class of mRNAs for which HuR may be the export adapter is heat shock mRNAs. The binding of HuR to one of these, hsp70 mRNA, has been documented (*69*). Among 18 stress-induced mRNAs surveyed, 15 exhibit discernable AREs in their 3′ UTRs (*57*). Our observation that the interaction of Trn2 with HuR is heat sensitive (Fig. 6) explains why HuR shuttling shifts to the CRM1 pathway after heat shock. As expected if HuR and its ligands serve as adapter, the export of hsp70 mRNA is inhibited not only by LMB (*69*) but also by the AP-NES peptide (*57*). We do not yet know whether HuR export switches to the CRM1 pathway upon exposure to other stress conditions; the subcellular distribution of hnRNP A1 has been observed to respond differentially to different types of stress (*74*).

An important advantage of using cell-permeable peptides to study mRNA export is that endogenous mRNAs are examined in living cells. We were surprised that the overall distribution of total poly(A)$^+$ RNA was not detectably perturbed by the presence of a single inhibitory peptide [or even a combination of two (Fig. 4) or three peptides (*57*)]. This observation demonstrates that the Ran-GTP gradient, which is essential for the normal export of many cellular RNAs and RNPs (*1*, *75*), is not being substantially disrupted by peptide treatment. We therefore conclude that the HNS-Trn2, NES-CRM1, and M9-Trn1 pathways are the principle export routes for only small groups of cellular mRNAs, whereas many others appear to be governed by the TAP export receptor (*26–30*). Because the M9 motif is conserved among many different hnRNP proteins (20, *66*), AP-M9 may target several pathways dependent on related hnRNP adapter proteins. The mechanism of action of the peptide inhibitors is most likely competition with adapter-receptor interactions, but they could act by abolishing an essential posttranslational modification of the corresponding adapter protein (e.g., phosphorylation). Use of peptides should allow the facile identification of the adapter-receptor pairs [e.g., Aly/REF-TAP (*8*, *26*, *27*, *30*)] that are dominant in the export of other mRNAs. It will be particularly interesting to learn how many mRNAs access alternative pathways and whether the route used varies in response to environmental conditions.

References and Notes

1. J. E. Dahlberg, E. Lund, *Curr. Opin. Cell Biol.* **10**, 400 (1998).
2. F. Stutz, M. Rosbash, *Genes Dev.* **12**, 3303 (1998).
3. I. W. Mattaj, L. Englmeier, *Annu. Rev. Biochem.* **67**, 265 (1998).
4. S. Nakielny, G. Dreyfuss, *Cell* **99**, 677 (1999).
5. B. R. Cullen, *Mol. Cell. Biol.* **20**, 4181 (2000).
6. M. J. Luo, R. Reed, *Proc. Natl. Acad. Sci. U.S.A.* **96**, 14937 (1999).
7. J. Zhao, L. Hyman, C. Moore, *Microbiol. Mol. Biol. Rev.* **63**, 405 (1999).
8. Z. Zhou *et al.*, *Nature* **407**, 401 (2000).
9. H. Le Hir, E. Izaurralde, L. E. Maquat, M. J. Moore, *EMBO J.* **19**, 6860 (2000).
10. M. Fukuda *et al.*, *Nature* **390**, 308 (1997).
11. M. Fornerod, M. Ohno, M. Yoshida, I. W. Mattaj, *Cell* **90**, 1051 (1997).
12. B. Ossareh-Nazari, F. Bachelerie, C. Dargemont, *Science* **278**, 141 (1997).
13. V. W. Pollard, M. H. Malim, *Annu. Rev. Microbiol.* **52**, 491 (1998).
14. M. Ohno, A. Segref, A. Bachi, M. Wilm, I. W. Mattaj, *Cell* **101**, 187 (2000).
15. J. H. Ho, G. Kallstrom, A. W. Johnson, *J. Cell Biol.* **151**, 1057 (2000).
16. N. Visa *et al.*, *Cell* **84**, 253 (1996).
17. S. Pinol-Roma, G. Dreyfuss, *Nature* **355**, 730 (1992).
18. W. M. Michael, M. Choi, G. Dreyfuss, *Cell* **83**, 415 (1995).
19. V. W. Pollard *et al.*, *Cell* **86**, 985 (1996).
20. M. C. Siomi *et al.*, *J. Cell Biol.* **138**, 1181 (1997).
21. E. Izaurralde *et al.*, *J. Cell Biol.* **137**, 27 (1997).
22. D. Gorlich, U. Kutay, *Annu. Rev. Cell. Dev. Biol* **15**, 607 (1999).
23. W. M. Michael, P. S. Eder, G. Dreyfuss, *EMBO J.* **16**, 3587 (1997).
24. Y. Huang, J. A. Steitz, *Mol. Cell* **7**, 899 (2001).
25. J. F. Caceres, G. R. Screaton, A. R. Krainer, *Genes Dev.* **12**, 55 (1998).
26. Y. Kang, B. R. Cullen, *Genes Dev.* **13**, 1126 (1999).
27. F. Stutz *et al.*, *RNA* **6**, 638 (2000).
28. P. Gruter *et al.*, *Mol. Cell* **1**, 649 (1998).
29. I. C. Braun, E. Rohrbach, C. Schmitt, E. Izaurralde, *EMBO J.* **18**, 1953 (1999).
30. J. P. Rodrigues *et al.*, *Proc. Natl. Acad. Sci. U.S.A.* **98**, 1030 (2001).
31. J. L. Veyrune, J. Hesketh, J. M. Blanchard, *Prog. Mol. Subcell. Biol.* **18**, 35 (1997).
32. S. C. Schiavi, J. G. Belasco, M. E. Greenberg, *Biochim. Biophys. Acta* **1114**, 95 (1992).
33. C. Y. Chen, A. B. Shyu, *Trends Biochem. Sci.* **20**, 465 (1995).
34. A. Jacobson, S. W. Peltz, *Annu. Rev. Biochem.* **65**, 693 (1996).
35. D. Antic, J. D. Keene, *Am. J. Hum. Genet.* **61**, 273 (1997).
36. C. M. Brennan, J. A. Steitz, *Cell. Mol. Life Sci.* **58**, 266 (2001).
37. W. J. Ma, S. Cheng, C. Campbell, A. Wright, H. Furneaux, *J. Biol. Chem.* **271**, 8144 (1996).
38. X. C. Fan, J. A. Steitz, *EMBO J.* **17**, 3448 (1998).
39. S. S. Peng, C. Y. Chen, N. Xu, A. B. Shyu, *EMBO J.* **17**, 3461 (1998).
40. X. C. Fan, J. A. Steitz, *Proc. Natl. Acad. Sci. U.S.A.* **95**, 15293 (1998).
41. T. H. Chen *et al.*, *Mol. Biol. Cell* **7**, 2045 (1996).
42. M. Mencinger, I. Panagopoulos, J. A. Contreras, F. Mitelman, P. Aman, *Biochim. Biophys. Acta* **1395**, 176 (1998).
43. C. M. Brennan, I. E. Gallouzi, J. A. Steitz, *J. Cell Biol.* **151**, 1 (2000).
44. I. E. Gallouzi *et al.*, *Proc. Natl. Acad. Sci. U.S.A.* **97**, 3073 (2000).
45. W. J. Ma, S. Chung, H. Furneaux, *Nucleic Acids Res.* **25**, 3564 (1997).
46. E. Vakalopoulou, J. Schaack, T. Shenk, *Mol. Cell. Biol.* **11**, 3355 (1991).
47. S. A. Tenenbaum, C. C. Carson, P. J. Lager, J. D. Keene, *Proc. Natl. Acad. Sci. U.S.A.* **97**, 14085 (2000).
48. A. E. Pasquinelli, M. A. Powers, E. Lund, D. Forbes, J. E. Dahlberg, *Proc. Natl. Acad. Sci. U.S.A.* **94**, 14394 (1997).
49. U. Fischer, J. Huber, W. C. Boelens, I. W. Mattaj, R. Luhrmann, *Cell* **82**, 475 (1995).
50. M. Bucci *et al.*, *Nature Med.* **6**, 1362 (2000).
51. D. Derossi, A. H. Joliot, G. Chassaing, A. Prochiantz, *J. Biol. Chem.* **269**, 10444 (1994).
52. D. Derossi *et al.*, *J. Biol. Chem.* **271**, 18188 (1996).
53. D. Derossi, G. Chassaing, A. Prochiantz, *Trends Cell Biol* **8**, 84 (1998).
54. M. J. May *et al.*, *Science* **289**, 1550 (2000).
55. M. H. Malim, D. F. McCarn, L. S. Tiley, B. R. Cullen, *J. Virol.* **65**, 4248 (1991).
56. M. H. Malim, S. Bohnlein, J. Hauber, B. R. Cullen, *Cell* **58**, 205 (1989).
57. I.-E. Gallouzi, J. A. Steitz, data not shown.
58. R. K. Ernst, M. Bray, D. Rekosh, M. L. Hammarskjold, *Mol. Cell. Biol.* **17**, 135 (1997).
59. T. J. Hope, X. J. Huang, D. McDonald, T. G. Parslow, *Proc. Natl. Acad. Sci. U.S.A.* **87**, 7787 (1990).
60. B. M. Peterlin, P. A. Luciw, P. J. Barr, M. D. Walker, *Proc. Natl. Acad. Sci. U.S.A.* **83**, 9734 (1986).
61. In situ hybridization was performed as described (*44*, *76*). The probe was a 3′ digoxigenin-labeled antisense oligonucleotide for the reporter CAT mRNA (complementary to nucleotides 619 to 660 relative to the translation start site), used at 5 ng/ml with a 1:200 dilution of sheep antibody to digoxigenin Fab-rhodamine. Visualization was with a Zeiss Axiophot 2 microscope. No signal was obtained when the fixed cells were treated with RNase before hybridization or with the secondary antibody alone (*57*).
62. P. Askjaer, T. H. Jensen, J. Nilsson, L. Englmeier, J. Kjems, *J. Biol. Chem.* **273**, 33414 (1998).
63. HeLa cells were seeded at 2×10^5 cells per cover slip 24 hours after transfection with either the hnRNP A1-Myc (*18*) (Fig. 1C, panels 1 to 6) or pp32-Flag (*43*) (Fig. 1C, panels 7 to 15) pcDNA3 expression vector. At least 12 hours later, mouse L929 cells [which had been pretreated for 30 min with cychloheximide (75 μg/ml)] were added at 3×10^5 per cover slip, and after 2 hours, AP peptides were introduced at 25 μM. One hour later, heterokaryon formation was initiated. After fusion, the cells were incubated in medium containing cychloheximide (100 μg/ml) and 25 μM peptide(s) for 3 hours before fixing and staining (*38*).
64. S. Pinol-Roma, S. A. Adam, Y. D. Choi, G. Dreyfuss, *Methods Enzymol.* **180**, 410 (1989).
65. M. E. Greenberg, E. B. Ziff, *Nature* **311**, 433 (1984).
66. M. C. Siomi *et al.*, *Mol. Cell. Biol.* **18**, 4141 (1998).
67. Tagged proteins were expressed and purified as de-

scribed: GST-HuR and GST-pp32 (*43*); GST-Trn1, GST-Trn2, and Myc-hnRNP A1 (plasmids encoding these proteins were a gift from S. Nakielny and G. Dreyfuss, University of Pennsylvania, Philadelphia, PA) (*18–20*).
68. Polyclonal antibody to Trn2 (αTm2) was generated as described (*43*) by injecting a rabbit with 500 μg of GST-Trn2. The αTm2 polyclonal and αTm1 monoclonal (D45, gift of G. Dreyfuss) (*19, 20*) antibodies exhibited no detectable cross reactivity by Western blotting of recombinant GST-Tm1 and GST-Tm2 proteins (*57*).
69. I. E. Gallouzi, C. M. Brennan, J. A. Steitz, *RNA* **7**, 1348 (2001).
70. A. Schneider-Gadicke *et al.*, *Cancer Res.* **48**, 2969 (1988).
71. P. A. Lazo, *Eur. J. Biochem.* **165**, 393 (1987).
72. N. S. Levy, S. Chung, H. Furneaux, A. P. Levy, *J. Biol. Chem.* **273**, 6417 (1998).
73. W. Wang *et al.*, *Mol. Cell. Biol.* **20**, 760 (2000).
74. W. van der Houven van Oordt *et al.*, *J. Cell Biol.* **149**, 307 (2000).
75. M. S. Moore, G. Blobel, *Trends Biochem. Sci.* **19**, 211 (1994).
76. S. R. Wente, G. Blobel, *J. Cell Biol.* **123**, 275 (1993).
77. Peptides were synthesized by standard Fmoc chemistry, purified, and analyzed by reverse-phase high-pressure liquid chromatography and mass spectrometry by the W. M. Keck Biotechnology Resource Center at Yale University School of Medicine.
78. Single-letter abbreviations for the amino acid residues are as follows: A, Ala; C, Cys; D, Asp; E, Glu; F, Phe; G, Gly; H, His; I, Ile; K, Lys; L, Leu; M, Met; N, Asn; P, Pro; Q, Gln; R, Arg; S, Ser; T, Thr; V, Val; W, Trp; and Y, Tyr.
79. C. Elfgang *et al.*, *Proc. Natl. Acad. Sci. U.S.A.* **96**, 6229 (1999).
80. HeLa and L929 cells were cultured as described (*43*).
81. To detect c-fos mRNA, HeLa cells were starved in media lacking serum for 48 hours; then 10% fetal bovine serum (GIBCO) was added for 1 hour to stimulate c-fos transcription. Peptides were added 3 hours before serum stimulation and were present until the cells were fixed 1 hour later for in situ hybridization. No signal was obtained when cells were not serum induced (*57*).
82. In situ hybridization was performed with a 3′ digoxigenin-labeled antisense deoxyoligonucleotide probe for *c-fos* mRNA (panels 1 to 8) or for DHFR (dihydrofolate reductase) mRNA (panels 9 to 12) or with oligo(dT)$_{40}$ (panels 13 to 20) to visualize total cellular poly(A)$^+$ RNA. The probes were complementary to nucleotides 288 to 328 [from the translation start site of c-fos (Calbiochem)] or to nucleotides 530 to 569 for DHFR (synthesized by the Keck Facility, Yale University) and were used at 5 ng/ml with a 1:200 dilution of sheep antibody to digoxigenin Fab-rhodamine (Boehringer). Identical results were obtained with probes for the 3′ UTR of *c-fos* (complementary to nucleotides 3363 to 3473; a gift from J.-L. Veyrune) or DHFR (nucleotides 898 to 937; Keck Facility). All mRNA-specific probes gave single bands on Northern blots (*57*).
83. ^{35}S-labeled proteins were produced by in vitro transcription-translation (*19*) of 1 mg of pcDNA3-HuR (*38*), pcDNA Myc-hnRNP A1 (*18*), or pHybLex-HNS [made by subcloning the Eco RI–Xho I fragment of pcDNA3-HuR into the Eco RI–Xho I restriction sites of the pHybLex vector (Invitrogen)] plasmid. Far-Western blotting was performed as described (*20*).
84. For the bottom two panels of Fig. 5A, 10 μg each of GST or the indicated GST fusion protein was incubated for 1 hour at 4°C with 40 μl of glutathione-Sepharose (Pharmacia) in 500 μl of binding buffer [50 mM tris-HCl, 400 mM NaCl, 5 mM MgOAc, leupeptin (2 μg/ml), pepstatin (2 μg/ml), and 0.5% aprotinin (pH 7.5)], also used for washing.
85. We are most grateful to C. Brennan for help in generating the antibody to Trn2 and for valuable discussions and suggestions. We G. G. Carmichael, K. T. Tycowski, L. B. Weinstein, T. S. McConnell, J. Lykke-Andersen, and T. Hirose for comments on the manuscript and many helpful suggestions. We express our gratitude to S. Nakielny and G. Dreyfuss for providing the Trn1, Trn2, and hnRNP A1 plasmids as well as the monoclonal antibody to Trn1 and to S. Pinol Roma for the antibody to hnRNP A1 (4B10). This work was supported by grant CA16038 from the NIH. J.S. is an investigator of the Howard Hughes Medical Institute.

24 July 2001; accepted 12 October 2001

REPORTS

Photoinduced Conversion of Silver Nanospheres to Nanoprisms

Rongchao Jin,[1] YunWei Cao,[1] Chad A. Mirkin,[1]* K. L. Kelly,[1] George C. Schatz,[1]* J. G. Zheng[2]

A photoinduced method for converting large quantities of silver nanospheres into triangular nanoprisms is reported. The photo-process has been characterized by time-dependent ultraviolet-visible spectroscopy and transmission electron microscopy, allowing for the observation of several key intermediates in and characteristics of the conversion process. This light-driven process results in a colloid with distinctive optical properties that directly relate to the nanoprism shape of the particles. Theoretical calculations coupled with experimental observations allow for the assignment of the nanoprism plasmon bands and for the first identification of two distinct quadrupole plasmon resonances for a nanoparticle. Unlike the spherical particles they are derived from that Rayleigh light-scatter in the blue, these nanoprisms exhibit scattering in the red, which could be useful in developing multicolor diagnostic labels on the basis not only of nanoparticle composition and size but also of shape.

Size provides important control over many of the physical and chemical properties of nanoscale materials, including luminescence, conductivity, and catalytic activity (*1*, *2*). Colloid chemists have gained excellent control over particle size for several spherical metal and semiconductor compositions, which has led to the discovery of quantum confinement in colloidal nanocrystals and to the use of such structures as probes for biological diagnostic applications, LED materials, lasers, and Raman spectroscopy–enhancing materials (*3–10*). However, the challenge of synthetically controlling particle shape has been met with limited success. Nevertheless, some physical and solid-state chemical deposition methods have been developed for making semiconductor and metal nanowires, nanobelts, and nanodots (*11–13*). Now, there are also a variety of methods for making rods with somewhat controllable aspect ratios using seeding approaches (*14*, *15*) and electrochemical (*16*, *17*) and membrane-templated syntheses (*18*). Less is known about bulk solution synthetic methods for nonspherical particles, although methods do exist for making colloidal samples of Pt cubes and pyramids (*19*) and PbSe, CdS, and Ni triangles (*20–22*). Trace quantities of Au and Ag nanoprisms have been observed as by-products of methods that predominately produce spheres (*23*, *24*). Promising recent work has resulted in methods for synthesizing $BaCrO_4$, CdSe, and Co nanorods and distributions of arrow-, teardrop-, and tetrapod-shaped CdSe nanocrystals (*25–28*).

All of these solution methods are based on thermal processes, and, in most cases with the exception of rods, they yield relatively small quantities of the desired particle shape. Thus, the development of bulk solution synthetic methods that offer shape control is of paramount importance if the full potential of these materials is to be realized. Herein, we report a photoinduced method for synthesizing large quantities of silver nanoprisms in high yield in the form of a colloidal suspension. This photo-mediated route has led to a colloid with distinctive optical properties that directly relate to the shape control.

In a typical experiment, spherical silver particles were prepared by injection of $NaBH_4$ solution (50 mM, 1 ml) to an aqueous solution of $AgNO_3$ (0.1 mM, 100 ml) in the presence of trisodium citrate (0.3 mM). Bis(*p*-sulfonatophenyl) phenylphosphine dihydrate dipotassium salt solution (BSPP) (5 mM, 2 ml) was subsequently added by drop-wise addition to the solution as a particle stabilizing agent. The system is then irradiated with a conventional 40-W fluorescent light (General Electric, Cleveland,

[1]Department of Chemistry and Institute for Nanotechnology, [2]Department of Materials Science and Engineering, Northwestern University, 2145 Sheridan Road, Evanston, IL 60208, USA.

*To whom correspondence should be addressed. E-mail: camirkin@chem.nwu.edu (experimental work) or schatz@chem.nwu.edu (theoretical work).